

Nicotine-induced Up-regulation and Desensitization of $\alpha 4\beta 2$ Neuronal Nicotinic Receptors Depend on Subunit Ratio*

Received for publication, March 31, 2004, and in revised form, June 22, 2004
Published, JBC Papers in Press, July 9, 2004, DOI 10.1074/jbc.M403537200

Gretchen Y. López-Hernández^{‡§}, Javier Sánchez-Padilla^{¶||}, Alejandro Ortiz-Acevedo[‡],
José Lizardi-Ortiz[‡], Janice Salas-Vincenty[‡], Legier V. Rojas^{**}, and José A. Lasalde-Dominicci^{‡ ††}

From the [‡]University of Puerto Rico, Department of Biology, P.O. Box 23360, San Juan, Puerto Rico 00931-3360,
[¶]Baylor College of Medicine, Division of Neuroscience, Houston, Texas 77030, and ^{**}Universidad Central del Caribe,
Department of Physiology, Bayamón, Puerto Rico 00916

Desensitization induced by chronic nicotine exposure has been hypothesized to trigger the up-regulation of the $\alpha 4\beta 2$ neuronal nicotinic acetylcholine receptor (nAChR) in the central nervous system. We studied the effect of acute and chronic nicotine exposure on the desensitization and up-regulation of different $\alpha 4\beta 2$ subunit ratios (1 α :4 β , 2 α :3 β , and 4 α :1 β) expressed in *Xenopus* oocytes. The presence of $\alpha 4$ subunit in the oocyte plasmatic membrane increased linearly with the amount of $\alpha 4$ mRNA injected. nAChR function and expression were assessed during acute and after chronic nicotine exposure using a two-electrode voltage clamp and whole-mount immunofluorescence assay along with confocal imaging for the detection of the $\alpha 4$ subunit. The 2 α :4:3 β :2 subunit ratio displayed the highest ACh sensitivity. Nicotine dose-response curves for the 1 α :4:4 β :2 and 2 α :4:3 β :2 subunit ratios displayed a biphasic behavior at concentrations ranging from 0.1 to 300 μ M. A biphasic curve for 4 α :4:1 β :2 was obtained at nicotine concentrations higher than 300 μ M. The 1 α :4:4 β :2 subunit ratio exhibited the lowest ACh- and nicotine-induced macroscopic current, whereas 4 α :4:1 β :2 presented the largest currents at all agonist concentrations tested. Desensitization by acute nicotine exposure was more evident as the ratio of $\beta 2$: $\alpha 4$ subunits increased. All three $\alpha 4\beta 2$ subunit ratios displayed a reduced state of activation after chronic nicotine exposure. Chronic nicotine-induced up-regulation was obvious only for the 2 α :4:3 β :2 subunit ratio. Our data suggest that the subunit ratio of $\alpha 4\beta 2$ determines the functional state of activation, desensitization, and up-regulation of this neuronal nAChR. We propose that independent structural sites regulate $\alpha 4\beta 2$ receptor activation and desensitization.

Neuronal nicotinic acetylcholine receptors (nAChRs)¹ belong to a superfamily of ligand-gated ion channels (e.g. γ -aminobu-

tyric acid, glutamate, 5-hydroxytryptamine, among others) and play an important role in modulating neurotransmitter release in distinct areas of the central and peripheral nervous system (1–5). Nicotine is the active ingredient of tobacco and specifically binds to nAChRs in the brain (3). One of the most remarkable effects of chronic nicotine exposure is the up-regulation of the $\alpha 4\beta 2$ subtype in the central nervous system (6–10). Another important effect of chronic nicotine exposure is the long lasting functional deactivation of nAChR receptor (11–17). Chronic nicotine exposure produces a loss of nicotinic functional activity as a result of rapid and persistent desensitization (11, 18–20). Desensitization induced by chronic exposure to nicotine has been hypothesized to trigger the up-regulation of the $\alpha 4\beta 2$ nAChR (3, 6, 21–23). The effect of chronic nicotine exposure on the activity of nAChR subtypes may be related to symptoms associated with nicotine addiction (3, 24, 25) such as tolerance, dependence, and withdrawal. In contrast to the aforementioned studies, a recent work suggests that the $\alpha 4\beta 2$ subtype expressed in the stable cell line K-177 functionally up-regulates with chronic nicotine exposure (26). The molecular mechanisms that underlie a possible link between desensitization, deactivation, and up-regulation of the $\alpha 4\beta 2$ subtype induced by chronic nicotine exposure remain unclear.

Previous studies have proposed that the subunit stoichiometry of the $\alpha 4\beta 2$ expressed in oocytes is ($\alpha 4$)₂($\beta 2$)₃ (27, 28). Various functional studies, however, suggest that ($\alpha 4$)₂($\beta 2$)₃ is not the only stoichiometry present in cells expressing this nAChR subtype. For instance, patch clamp recordings from oocytes expressing the $\alpha 4\beta 2$ nAChR have demonstrated that single channel conductance depends on the α : β ratio of the mRNA injected into the oocyte (29). When the relative levels of expression of the $\alpha 4$ and $\beta 2$ were varied by nuclear injection of three α : β ratios into *Xenopus* oocytes, different sensitivities to acetylcholine and *d*-tubocurarine were obtained using voltage clamp recording (30). These results suggest that the subunit stoichiometry of functional heteromeric $\alpha 4\beta 2$ nAChRs is not limited to ($\alpha 4$)₂($\beta 2$)₃. Furthermore, a recent work by Nelson *et al.* (31) reported two functional types of $\alpha 4\beta 2$ nAChRs expressed in human embryonic kidney cells. These investigators found that the predominant subunit stoichiometry of $\alpha 4\beta 2$ nAChRs expressed in human embryonic kidney cells was ($\alpha 4$)₃($\beta 2$)₂, yet overnight nicotine exposure increased the proportion of nAChRs with a ($\alpha 4$)₂($\beta 2$)₃ stoichiometry.

In this study, we examine the effect of acute and chronic exposure to nicotine on the desensitization and up-regulation of different subunit ratios of $\alpha 4$: $\beta 2$ expressed in *Xenopus* oocytes. The desensitization and up-regulation of three subunit ratios of $\alpha 4\beta 2$ nAChR were assessed using a two-electrode voltage clamp in *Xenopus* oocytes, and whole-mount immunofluorescence assay and confocal imaging were used for surface detec-

* This work was supported by National Institute of Health Grants 2R01GM56371-05, NCRN S13705-01, and GM08102-27 and Fondos Institucionales para la Investigacion institutional funds. The costs of publication of this article were defrayed in part by the payment of page charges. This article must therefore be hereby marked "advertisement" in accordance with 18 U.S.C. Section 1734 solely to indicate this fact.

§ Supported by the Research Initiative for Scientific Enhancement-Minority Biomedical Research Support-National Institutes of Health program (Grant 5R25GM61151).

|| Supported by the Minority Access to Research Careers-Minority Biomedical Research Support-National Institutes of Health program.

†† To whom correspondence should be addressed: Dept. of Biology, University of Puerto Rico, P.O. Box 23360, JGD-114, San Juan, PR 00931. Tel.: 787-764-0000 (ext. 2765); Fax: 787-753-3852; E-mail: joseal@coqui.net.

¹ The abbreviations used are: nAChR, neuronal nicotinic acetylcholine receptor; ACh, acetylcholine; ANOVA, analysis of variance.

tion of $\alpha 4$ neuronal subunits. Our data suggest that different $\alpha 4\beta 2$ subunit ratios expressed in *Xenopus* oocytes can produce differential rates of desensitization and up-regulation, thus implying that subunit assembly of this nAChR is critical in these two processes.

EXPERIMENTAL PROCEDURES

In Vitro Synthesis of mRNA and Oocyte Microinjection—Subunit mRNA was synthesized *in vitro* from linearized pGEMHE plasmid templates of *Rattus norvegicus* cDNA coding for $\alpha 4$ and $\beta 2$ nAChR subunits using the mMessage mMachine RNA transcription kit (Ambion, Austin, TX). mRNA mixtures of $\alpha 4$ and $\beta 2$ subunits were prepared at 1 μg :4 μg , 2 μg :3 μg , and 4 μg :1 μg α : β ratios. The mRNA mixture was microinjected using a displacement injector (Drummond Instruments, Broomhall, PA) into stage V and VI oocytes that had been extracted, incubated in collagenase Type 1A (Sigma), and defolliculated by manual dissection. The injected oocytes were incubated at 19 °C for 3 days in 0.5 \times Leibovitz's L-15 medium (Invitrogen) supplemented with 400 $\mu\text{g}/\text{ml}$ bovine serum albumin, 119 mg/ml penicillin, 200 mg/ml streptomycin, and 110 mg/ml pyruvic acid. Electrophysiological experiments were performed after the third day of mRNA injection.

Membrane Isolation from *Xenopus* Oocytes for Immunoblot Assay—Four batches of oocytes (~30–40 oocytes/batch) were used for each immunoblot assay. Three batches were microinjected with different $\alpha 4$: $\beta 2$ subunit ratios, and one batch was not injected (control). The number of oocytes was kept constant for each experiment. Membrane isolation was performed 3 days after microinjection as described by Ohlsson *et al.* (32) but with minor modifications. Briefly, a two-phase sucrose gradient was prepared with 1.5 and 0.3 M sucrose buffers (20 mM Tris-Cl, pH 7.6, 50 mM KCl, 10 mM MgCl₂, 2 mM β -mercaptoethanol, 1 mM EGTA, and the protease inhibitor mixture III), at a 1:2 ratio, respectively, in a 1.5-ml microtube. The inhibitor mixture was purchased from Calbiochem-Novabiochem, and the rest of the reagents were purchased from Sigma-Aldrich. The oocytes from each batch were manually disrupted with forceps, layered at the upper phase of the separation medium, and then centrifuged for 20 min at 12,000 $\times g$ (4 °C). The interface between the phases containing the membranes was removed, washed (5.0 mM HEPES, pH 7.4, 160 mM NaCl, and protease inhibitor mixture III), and centrifuged for 10 min at 3000 $\times g$ (4 °C). The wash buffer was removed, the pellet was resuspended in 400 μl of 4% SDS loading buffer and sonicated, divided into 40- μl aliquots, and stored at -80 °C.

Immunoblot Assay—40 μl of membrane solution were separated using SDS-PAGE (5% stacking and 10% running gel) and transferred to a nitrocellulose membrane (Bio-Rad). Membranes were blocked for 1 h at room temperature with 5% nonfat dry milk in Tris-buffered saline (20 mM Tris-Cl, pH 7.6, 137 mM NaCl, and 0.1% Tween 20). Membranes were incubated overnight at 4 °C with 100 μl of an antibody raised against the $\alpha 4$ subunit (AChR $\alpha 4$ -A-20; Santa Cruz Biotechnology, Santa Cruz, CA). Bound antibodies were detected with horseradish peroxidase-conjugated anti-goat (Kirkegaard and Perry Laboratories) and visualized using enhanced chemiluminescent detection (Amersham Biosciences). The immunoreactive bands were quantified using a GS800 calibrated densitometer and Quantitative One version 4 software (Bio-Rad). An equal and representative area of each band was selected, measured, and then normalized using a nonspecific band, which was consistently present in all blots. The identity of the band was determined by the blocking peptide AChR $\alpha 4$ -P (Santa Cruz Biotechnology). All of the reagents used were purchased from Sigma-Aldrich.

Electrophysiological Characterization of $\alpha 4\beta 2$ Subunit Ratios—Oocytes injected with the mRNA transcripts of $\alpha 4$ and $\beta 2$ at a ratio of 1 α :4 β , 2 α :3 β , or 4 α :1 β were characterized using a two-electrode voltage clamp. Acetylcholine (ACh) and nicotine-induced currents were recorded at 20 °C 3 days after mRNA injection with a GeneClamp 500B Amplifier (Axon Instruments, Foster City, CA). Electrodes were filled with 3 M KCl and had a resistance of less than 2 megaohms. Impaled oocytes in the recording chamber were continuously perfused at a rate of 0.75 ml/sec with MOR2 buffer (115 mM NaCl, 2.5 mM KCl, 5 mM HEPES, 1 mM Na₂HPO₄, 0.2 mM CaCl₂, 5 mM MgCl₂, and 0.5 mM EGTA, pH 7.4). All the reagents used were purchased from Sigma-Aldrich. For dose-response curves, each oocyte was held at a membrane potential of -70 mV. Membrane currents were digitized using the DigiData 1200 interface (Axon Instruments) filtered at 2 kHz during recording. The Whole Cell Program 2.3 (provided by Dr. J. Dempster, University of Strathclyde) running on a Pentium III-based computer was used for data acquisition. Data analysis was performed using Prism 3.0 (Graphpad Software, San Diego, CA). Dose-response data for the $\alpha 4\beta 2$ combi-

nation were collected using seven ACh or nicotine concentrations (0.1, 1, 3, 10, 30, 100 and 300 μM). The data were fit using one- and two-component sigmoidal dose-response equations, $Y = I/I_{\text{maxBottom}} + (I/I_{\text{maxTop}} - I/I_{\text{maxBottom}})/(1 + 10^{((\text{LogEC}_{50} - X) \times \text{Hillslope}))}$ and $Y = I/I_{\text{maxBottom}} + [(I/I_{\text{maxTop}} - I/I_{\text{maxBottom}}) \times \text{Fraction}/(1 + 10^{((\text{LogEC}_{50,1} - X) \times \text{Hillslope}_1)})] + [(I/I_{\text{maxTop}} - I/I_{\text{maxBottom}}) \times (1 - \text{Fraction})/(1 + 10^{((\text{LogEC}_{50,2} - X) \times \text{Hillslope}_2)})]$, respectively, where X is the logarithm of concentration and Y is the response. The protocol followed in the experiments involving acute nicotine exposure consisted of measuring the current induced by six consecutive applications of 300 μM ACh. Between each ACh application, the oocyte was either washed with MOR2 (control) or with nicotine-containing (0.3, 1.0, or 10 μM) MOR2 for 2 min. That is, a total of five washes for the six ACh applications. We chose 300 μM ACh based on the maximal response observed in all subunit ratios using this ACh concentration. To calculate percent recovery, oocytes were washed for 20 min with nicotine-free MOR2 buffer after the last nicotine wash. We also conducted experiments to assess the effect of chronic nicotine exposure on the ACh- and nicotine-induced responses for all three subunit ratios studied. To that end, we obtained ACh and nicotine dose-response curves (0.1, 1, 3, 10, 30, 100, and 300 μM) before and after prolonged nicotine incubation. For this nicotine incubation, oocytes were placed in L-15 medium supplemented with nicotine at a final concentration of 1 μM for 24 h. Subsequently, oocytes were washed for 5 mins by perfusing them with MOR2 buffer. Finally, ACh and nicotine dose-responses were determined as was conducted prior to the chronic nicotine incubation. The average peak currents of $\alpha 4\beta 2$ nAChRs from the three different α : β ratios were measured before and after 1 μM nicotine exposure. The peak currents were obtained at 300 μM ACh and 30 μM nicotine. Data are expressed as means \pm S.E. One-way ANOVA was performed using Prism 3.0. Results were compared with two-tailed Student's t test using Prism 3.0.

Immunofluorescence Assay for $\alpha 4\beta 2$ Neuronal nAChR—*Xenopus* oocytes were injected with the mRNA transcripts of $\alpha 4$ and $\beta 2$ in subunit ratios of 1 α :4 β , 2 α :3 β , or 4 α :1 β . Oocytes were incubated for 72 h (3 days) in L-15 medium supplemented with antibiotics and antimycotics. On the third day of injection, 300 μM ACh-induced currents were measured using the two-electrode voltage clamp technique. Oocytes to be compared were paired according to their similar current profile, *i.e.* with no more than 400 nA difference. Nicotine pre-incubation consisted of 24 h in L-15 medium supplemented with 1 μM nicotine. Non-incubated oocytes were placed in L-15 nicotine-free solution. Following chronic exposure to nicotine, incubated and non-incubated oocytes were dehydrated with Me₂SO:methanol solution mixture, rehydrated with MOR2 buffer without EGTA (115 mM NaCl, 2.5 mM KCl, 5 mM HEPES, 1 mM Na₂HPO₄, 0.2 mM CaCl₂, and 5 mM MgCl₂, pH 7.4), and then fixed in 4% paraformaldehyde. Oocytes were then incubated in goat serum blocking solution prior to antibody treatment. They were then incubated overnight with a monoclonal antibody against the extracellular domain of the rat $\alpha 4$ nAChR subunit (mAb299, purchased from Covance Co.) and then washed with MOR2 solution. Finally, oocytes were incubated overnight with a secondary antibody conjugated to fluorescein isothiocyanate (Kirkegaard and Perry Laboratories). Goat serum and antibodies were diluted in MOR2 buffer supplemented with 0.1% Triton X-100.

All images were acquired using a Zeiss LSM 510 confocal microscope (Carl Zeiss, Inc., Thornwood, NY) equipped with a Plan-Neofluar 10 \times /0.3 objective. Multiple images (optical slices; ≈ 5 μm thick) were acquired to construct Z stacks from each oocyte. Pinhole size, photomultiplier gain and offset, pixel size, and data depth settings were kept the same for all the images acquired in each experiment. Autofluorescence and background noise intensity values were obtained from non-injected oocytes in each experiment. We used MetaMorph® (Universal Imaging Corporation, Downingtown, PA) to process each image. The threshold function was used to eliminate the fluorescence intensity values from pixels not contributing to the image (*e.g.* background and autofluorescence). In addition, the same area (μm^2) was selected for each control-experimental pair analyzed to make comparisons between optical slices. The total fluorescence intensity value was then calculated from each optical slice from the control and nicotine-incubated oocyte.

RESULTS

Estimation of the Amount of $\alpha 4$ Subunit in the Plasmatic Membrane—The plasmatic membranes from different batches of oocytes injected with three different $\alpha 4\beta 2$ subunit ratios (1 α :4 β , 2 α :3 β , or 4 α :1 β) were isolated and homogenized, and the level of $\alpha 4$ subunit was analyzed by Western blotting (see "Experimental Procedures"). The identity of the band was determined by the molecular mass (≈ 67 kDa, Fig. 1A) and the

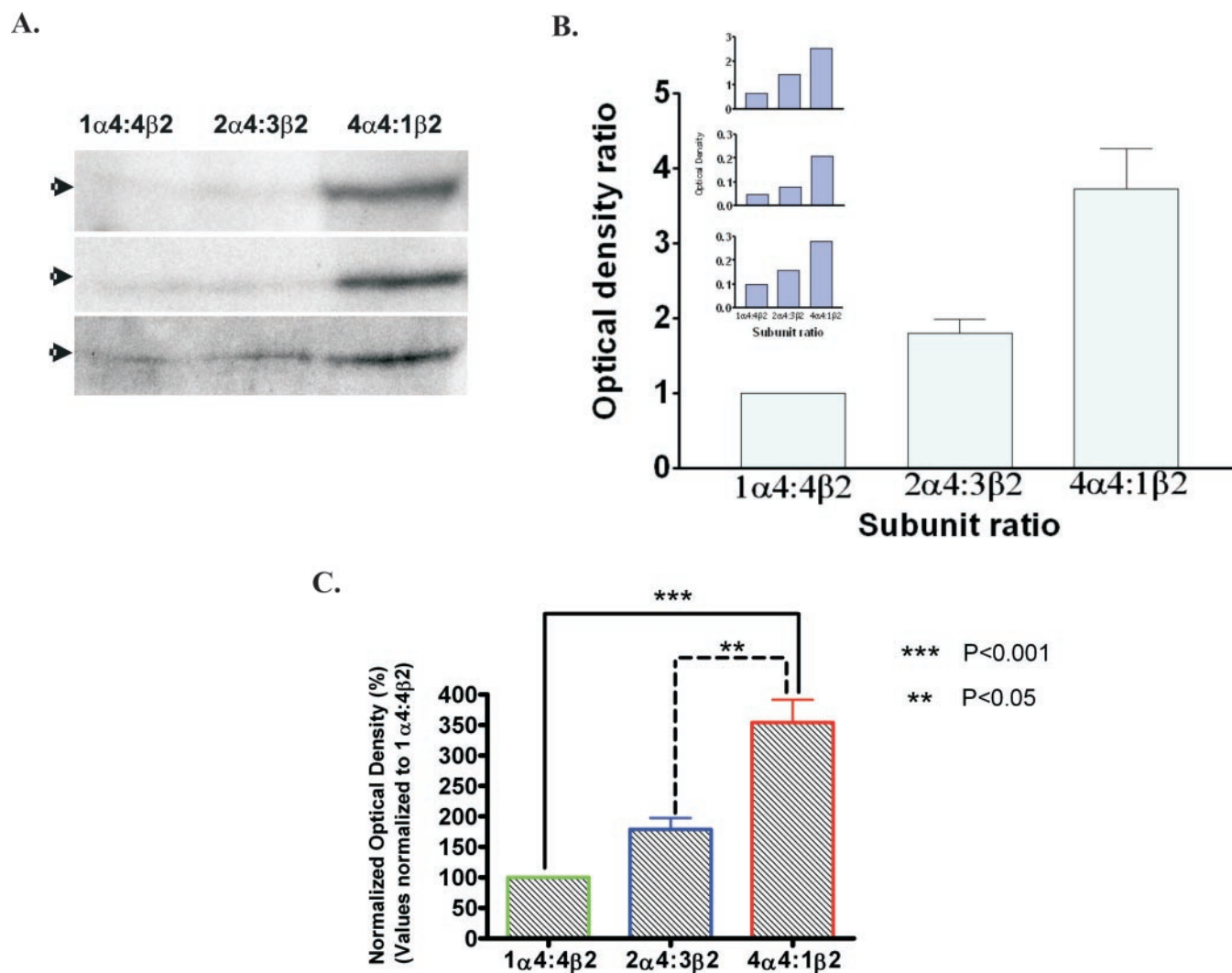


FIG. 1. Optical density ratios of $\alpha 4$ subunit in the membrane of oocytes microinjected with three different mRNA $\alpha 4:\beta 2$ ratios. *A*, Western blots from three different batches of *Xenopus* oocytes (30–40 oocytes/batch) injected with three different $\alpha:\beta$ ratios (1:4, 2:3, and 4:1). The arrows identify the ~ 67 -kDa bands corresponding to the $\alpha 4$ subunit. *B*, bar graphs illustrating the optical density magnitudes for each subunit ratio. The inset (dark blue bars) illustrates the optical density magnitudes calculated from the three Western blots (WB) shown in *A* ($1\alpha 4:4\beta 2$, $2\alpha 4:3\beta 2$, $4\alpha 4:1\beta 2$; WB1: 0.66, 1.43, 2.52; WB2: 0.10, 0.16, 0.28; WB3: 0.05, 0.08, and 0.2). The results for each independent experiment were normalized with respect to the $1\alpha 4:4\beta 2$ ratio (optical density ratio), averaged, and presented in the light blue bars as mean \pm S.E. Because the latter ratio is based on $1\alpha 4:4\beta 2$, this ratio becomes unity and has no S.E. *C*, bar graphs showing the results from one-way ANOVA with Bonferroni's multiple comparison test of the normalized optical density percent values.

disappearance of the band produced by the blocking peptide (data not shown). The results for three independent experiments were normalized with respect to the $1\alpha 4:4\beta 2$ subunit ratio (left lane in Fig. 1A). The mean and S.E. of the optical density ratios were 1.0 ± 0.0 , 1.8 ± 0.3 , and 3.7 ± 0.9 for $1\alpha 4:4\beta 2$, $2\alpha 4:3\beta 2$, and $4\alpha 4:1\beta 2$, respectively. Fig. 1B shows that the optical density magnitudes increased linearly in proportion to the ratio of $\alpha 4:\beta 2$ injected into oocytes. A one-way ANOVA with a Bonferroni post-test showed that the percent values of the normalized optical densities of the three subunit ratios were significantly different (Fig. 1C). A 0.92 ± 0.04 slope ($R^2 = 0.998$) was obtained from linear regression analysis, indicating that the presence of the $\alpha 4$ subunit in the plasmatic membranes increased linearly with the amount of the $\alpha 4$ mRNA subunit injected into the oocytes.

Subunit Ratio and Nicotine-induced Desensitization—Fig. 2 illustrates the effect of acute nicotine exposure on the response to six consecutive applications of $300 \mu\text{M}$ ACh to oocytes injected with three $\alpha 4\beta 2$ mRNA subunit ratios ($1\alpha 4:\beta 2$, $2\alpha 4:3\beta 2$, or $4\alpha 4:1\beta 2$). For the experimental conditions, nicotine (0.3, 1.0, or $10.0 \mu\text{M}$) was acutely applied between each ACh application as

described under “Experimental Procedures.” Fig. 2A (from left to right) illustrates representative current traces of control experiments with nicotine-free washes between ACh pulses for the three subunit ratios. In the absence of acute nicotine, ACh does not produce a significant current loss in the $1\alpha 4:4\beta 2$ and $4\alpha 4:1\beta 2$ subunit ratios; however, in the $2\alpha 4:3\beta 2$ subunit ratio, ACh produces a mild desensitization (30% of current lost) after six consecutive ACh applications (Fig. 2F). Fig. 2, B–D, depicts the results of acute nicotine exposure on the ACh-induced currents. The nicotine concentrations used were 0.3 (B), 1.0 (C) and $10 \mu\text{M}$ nicotine (D). At all nicotine concentrations tested, $1\alpha 4:4\beta 2$ (green) displayed the largest progressive loss in macroscopic current during acute nicotine exposure, whereas $4\alpha 4:1\beta 2$ (red) displayed the lowest loss of macroscopic current (Fig. 2, E and F). For example, at $1.0 \mu\text{M}$ acute nicotine exposure the percentages of current lost from their original macroscopic current were 72% for $1\alpha 4:4\beta 2$ (green), 66% for $2\alpha 4:3\beta 2$ (blue), and 51% for $4\alpha 4:1\beta 2$ (red) (Fig. 2F). The mean values for the amount of current lost after acute nicotine exposure using $1.0 \mu\text{M}$ nicotine were significantly different ($p < 0.05$) for the three $\alpha 4\beta 2$ subunit ratios. Fig. 2, E and F, demonstrate that the

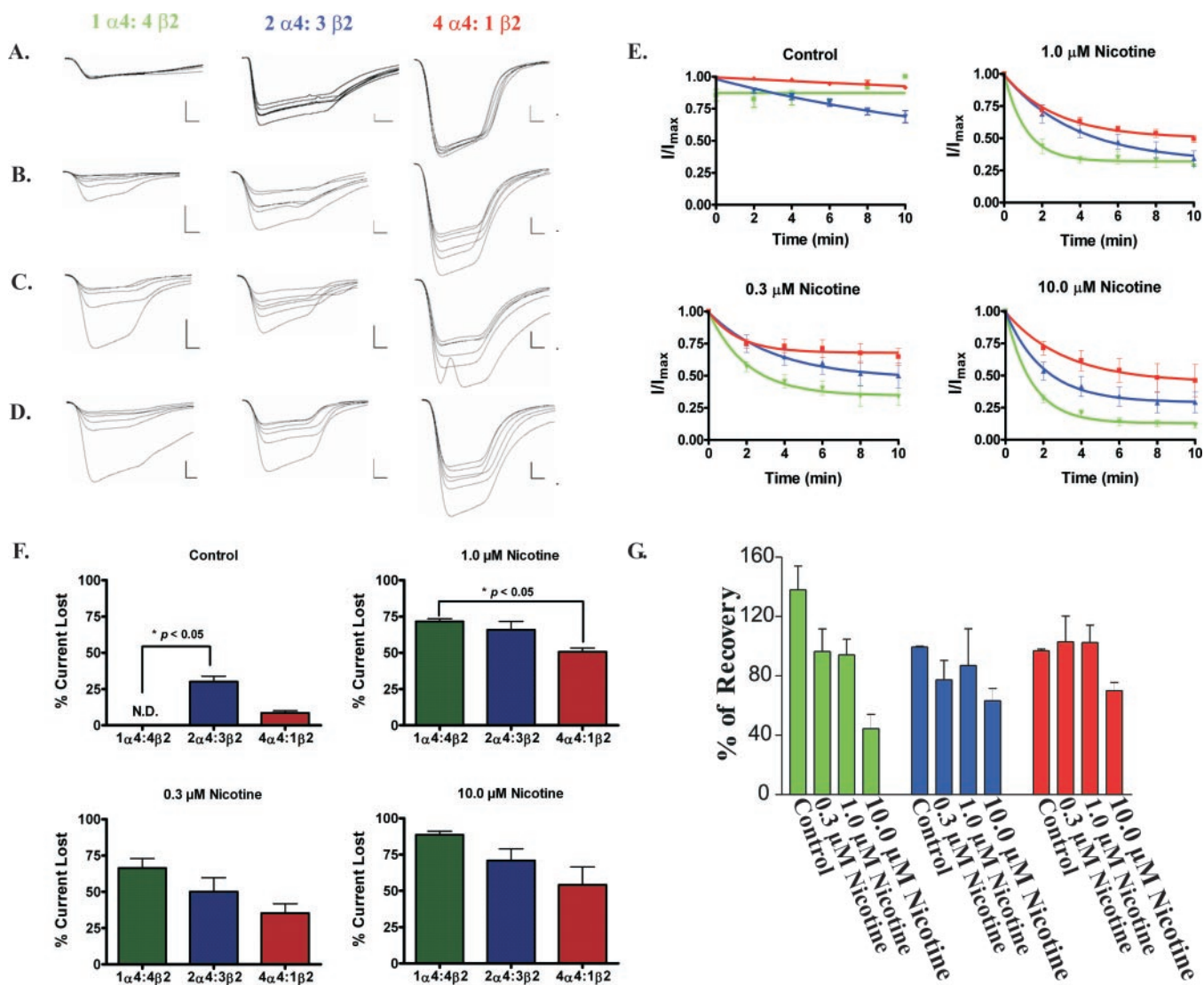


FIG. 2. Dependence of nicotine-induced desensitization of the $\alpha 4\beta 2$ nAChR subtype on subunit ratio. A, family of current traces (from left to right) for the three $\alpha 4\beta 2$ subunit ratios representing the response to six consecutive applications of $300 \mu\text{M}$ ACh using nicotine-free recording solution between ACh pulses (control experiment). B–D, family of current traces induced by six consecutive ACh applications ($300 \mu\text{M}$). Between each ACh pulse the oocytes were washed with nicotine-containing solution (0.3 , 1.0 , or $10.0 \mu\text{M}$, respectively) for 2 min (a total of five nicotine washes for six ACh applications). A–D, calibration bars are shown at the right of each current family, 250 nA (vertical bar) and 4 s (horizontal bar). E, graphs illustrating the ACh-induced response decay with respect to time of nicotine exposure for $\alpha 4\beta 2$ subunit ratios; $1\alpha 4:4\beta 2$ in green, $2\alpha 4:3\beta 2$ in blue, and $4\alpha 4:1\beta 2$ in red. F, bar graphs illustrating the average percent of ACh response lost as result of acute nicotine exposure for each subunit ratio. Statistical analysis was performed using one-way ANOVA with Bonferroni post-test. N.D., nondetectable current. G, percent recovery of the ACh-induced response after 20 min of nicotine withdrawal. Data were obtained from 3 to 11 oocytes.

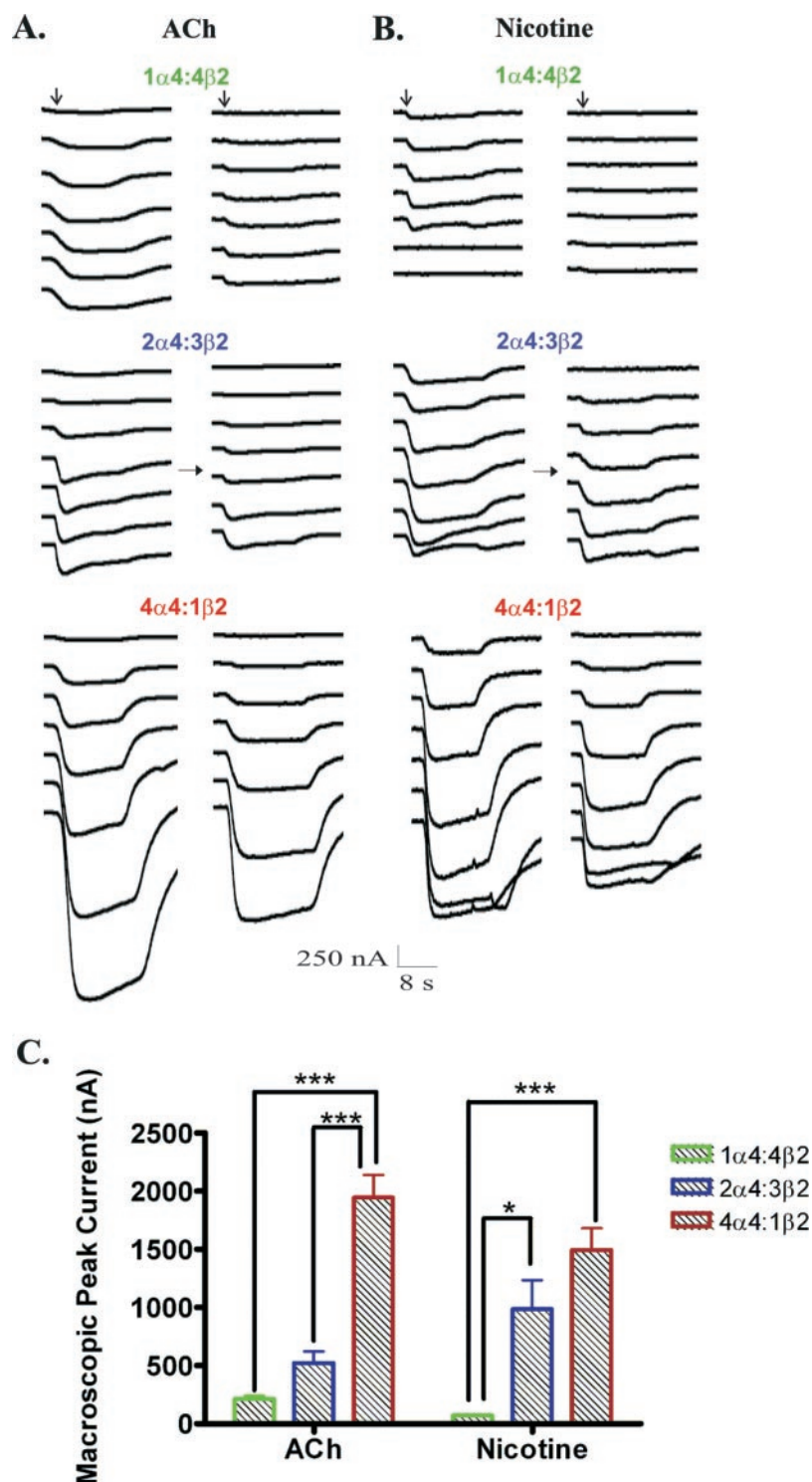
ACh-induced response decreases as the nicotine concentration increases. The current loss during acute exposure was probably caused by nAChR desensitization.

The amount of recovery from acute exposure (see “Experimental Procedures”) was measured for the three subunit ratios at each nicotine concentration (Fig. 2G). One-way ANOVA analysis showed that the means of the amount of current recovered after acute nicotine exposure were not significantly different between subunit ratios. After acute exposure to $1.0 \mu\text{M}$ nicotine, the percentages of current recovered were 94 ± 10 , 87 ± 25 , and 102 ± 12 for $1\alpha 4:4\beta 2$, $2\alpha 4:3\beta 2$, and $4\alpha 4:1\beta 2$, respectively. Statistical analysis showed that the mean values for recovered current were not significantly different ($p = 0.7726$); therefore, these data suggest that the percent recovery from acute nicotine exposure is independent of subunit ratio.

Activation Properties of the Different $\alpha 4\beta 2$ Subunit Ratios before Chronic Nicotine Incubation—The activation properties of oocytes expressing different $\alpha 4:\beta 2$ subunit ratios were evaluated using two-electrode voltage clamp recording. To this end,

we measured the current response to seven ACh and nicotine concentrations. In all oocytes tested, the $1\alpha 4:4\beta 2$ subunit ratio showed the lowest ACh (Fig. 3A, left traces) and nicotine-induced macroscopic currents (Fig. 3B, left traces). In contrast, $4\alpha 4:1\beta 2$ presented the largest currents at all agonist concentrations tested. The average ACh- and nicotine-induced macroscopic peak currents before chronic nicotine incubation are presented in Fig. 3C. One-way ANOVA (Bonferroni post-test) results demonstrate that the average macroscopic peak currents for the three subunit ratios studied are significantly different, with $4\alpha 4:1\beta 2$ being the subunit ratio displaying the largest ACh- and nicotine-induced responses. The corresponding dose-response curves for ACh and nicotine are shown in Fig. 4 in blue. The EC_{50} values obtained for ACh and nicotine are very consistent with those reported previously for the wild type receptor (33). ACh dose-response curves were fitted using a single Hill equation and a two-component Hill equation. A better fit was obtained using the two-component equation for the $4\alpha 4:1\beta 2$ subunit ratio (Fig. 4, top panel). The ACh EC_{50}

FIG. 3. Effect of chronic nicotine exposure on $\alpha 4\beta 2$ subunit ratios expressed in *Xenopus* oocytes. Voltage clamp recording was used to determine the response of the three $\alpha 4\beta 2$ subunit ratios to several ACh (A) or nicotine (B) concentrations (0.1, 1, 3, 10, 30, 100, and 300 μM) before and after chronic nicotine exposure. Vertical black arrows mark the time of agonist application. Panels A and B, left side, show the family of currents for the control experiments (without chronic nicotine incubation). Horizontal black arrows represent 24 h of 1.0 μM nicotine incubation. After chronic nicotine treatment and prior to voltage clamp recording, oocytes were washed for 5 mins by perfusing with MOR2 buffer. Panels A and B, right side, illustrate the currents after chronic nicotine incubation. C, bar graphs illustrating the difference in peak current magnitude between the $\alpha 4\beta 2$ subunit ratios using ACh or nicotine as agonists. The peak currents were obtained at 300 μM ACh and 30 μM nicotine. Statistical analysis was performed using two-way ANOVA with Bonferroni's multiple comparison test (*, $p < 0.05$; ***, $p < 0.001$). Data were obtained from 6 to 11 oocytes.



values determined for 1 $\alpha 4$:4 $\beta 2$ and 2 $\alpha 4$:3 $\beta 2$ subunit ratios were $1.4 \pm 1.1 \mu\text{M}$ and $0.9 \pm 1.5 \mu\text{M}$, respectively (Table I, see Controls). The estimated ACh EC_{50} values for the 4 $\alpha 4$:1 $\beta 2$ subunit ratio were 4.0 ± 5.2 and $52.2 \pm 0.2 \mu\text{M}$ (Table I, see Controls). The ACh EC_{50} value for the 4 $\alpha 4$:1 $\beta 2$ subunit ratio was significantly different from the other two subunit ratios ($p = 0.0001$). The dose-response curves for nicotine showed a bell-shaped profile for the 1 $\alpha 4$:4 $\beta 2$ and 2 $\alpha 4$:3 $\beta 2$ subunit ratios at nicotine concentrations ranging from 0.1 to 300 μM , (Fig. 4, lower panel in blue); however, the 4 $\alpha 4$:1 $\beta 2$ did not exhibit a biphasic response at these concentrations. 4 $\alpha 4$:1 $\beta 2$ exhibited a biphasic behavior when the nicotine concentration was in-

creased to 3 mM (Fig. 4, panel insert). One-way ANOVA analysis showed no significant difference among the mean EC_{50} values for nicotine for the three subunit ratios (Table I). No significant difference in the Hill slope was observed between the three subunit ratios when using either ACh or nicotine as agonists (Table I, see Controls).

Chronic Nicotine Exposure and Activation of Different $\alpha 4\beta 2$ Subunit Ratios—To evaluate the effect of chronic nicotine exposure on the functional activation of oocytes expressing different $\alpha 4$: $\beta 2$ subunit ratios, their response to several concentrations of ACh and nicotine (0.1–300 μM) were measured after 24 h of incubation in 1.0 μM nicotine (Fig. 3, A and B, right

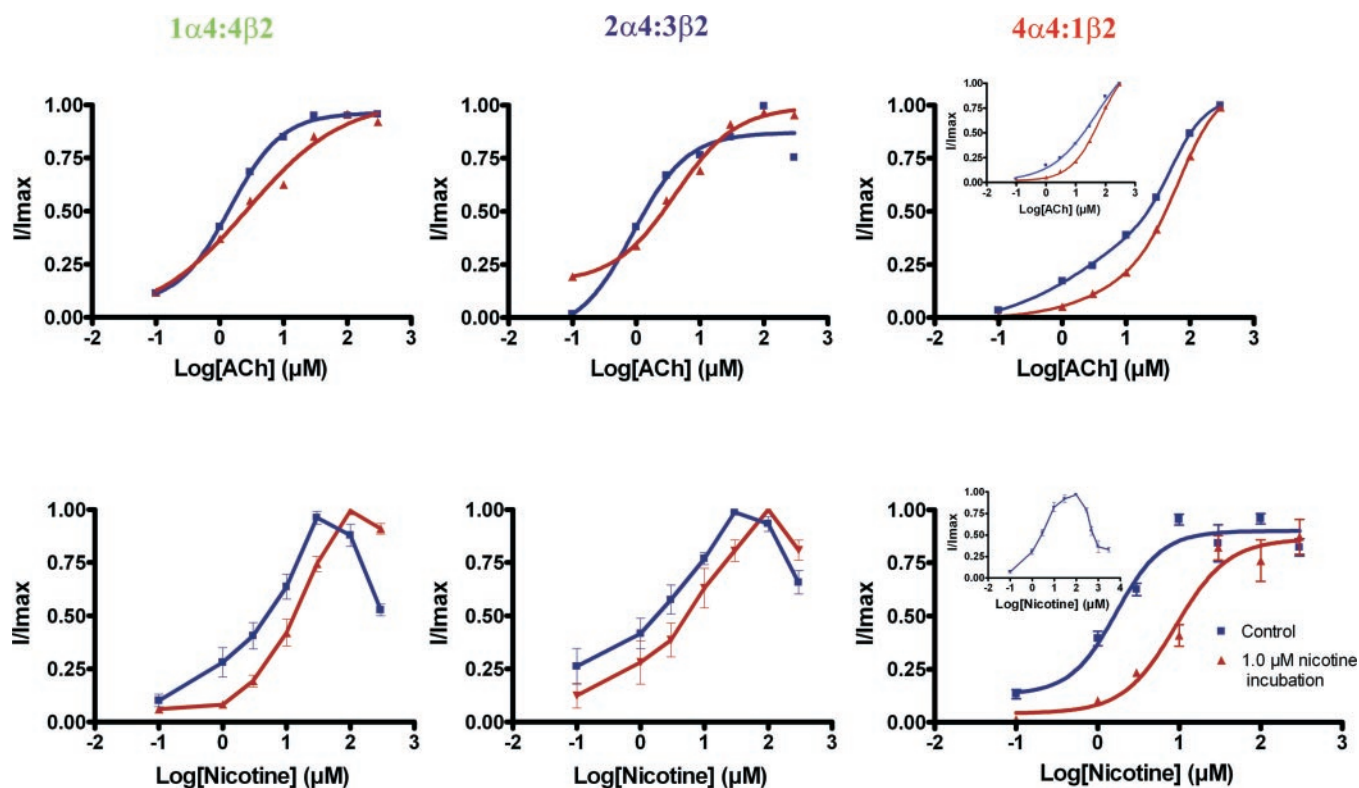


FIG. 4. Dependence of the functional response to ACh and nicotine on the mRNA subunit ratio injected into *Xenopus* oocytes. Agonist-induced responses were normalized to the maximum response (I/I_{\max}). Top panels show the dose-response relationships using ACh as agonist for each subunit ratio, and the nicotine dose-response relationships are presented in the bottom panels (0.1, 1, 3, 10, 30, 100, and 300 μM for each agonist). ACh dose-response curves were fitted using a single Hill equation and a two-component Hill equation. A better fit was obtained using the two-component equation for the 4 $\alpha 4$:1 $\beta 2$ subunit ratio. The inset in the ACh dose-response for 4 $\alpha 4$:1 $\beta 2$ (top panel) corresponds to the one-component fitting. Nicotine dose-response demonstrates a biphasic behavior for 1 $\alpha 4$:4 $\beta 2$ and 2 $\alpha 4$:3 $\beta 2$ using 0.1, 1, 3, 10, 30, 100, and 300 μM concentrations. 4 $\alpha 4$:1 $\beta 2$ exhibited a biphasic behavior when the nicotine concentration was increased to 3 mM (lower panel inset). Data from control oocytes (in the absence of chronic nicotine incubation) are shown in blue, whereas the results after 24 h 1.0 μM nicotine incubation are shown in red. Dose-response curves for both agonists represent the average and standard error of the mean for 6–11 oocytes.

TABLE I
Functional effects of chronic nicotine exposure as a function of $\alpha 4\beta 2$ subunit ratio

* indicates $p < 0.05$, n indicates the number of oocytes tested, 300 μM ACh and 30 μM nicotine were used to estimate peak currents.

| Subunit ratio | 1 $\alpha 4$:4 $\beta 2$ | 2 $\alpha 4$:3 $\beta 2$ | 4 $\alpha 4$:1 $\beta 2$ | |
|---|-----------------------------|-----------------------------|------------------------------|-----------------------------|
| Peak current at 300 μM ACh (nA \pm S.E.) | | | | |
| Control | 211 \pm 28* | 522 \pm 99* | 1943 \pm 195* | |
| 1 μM nicotine incubation | 67 \pm 10* ($n = 15$) | 283 \pm 68* ($n = 16$) | 1209 \pm 173* ($n = 39$) | |
| Peak current at 30 μM nicotine (nA \pm S.E.) | | | | |
| Control | 69 \pm 10* | 984 \pm 251* | 1493 \pm 188* | |
| 1 μM nicotine incubation | 23 \pm 3* ($n = 12$) | 480 \pm 146* ($n = 18$) | 533 \pm 109* ($n = 9$) | |
| EC_{50} ACh (μM \pm S.E.) | | | | |
| Control | 1.4 \pm 1.1 | 0.9 \pm 1.5* | 4.0 \pm 5.2 | 52.2 \pm 0.2 |
| 1 μM nicotine incubation | 2.7 \pm 1.6 ($n = 8$) | 4.1 \pm 1.3* ($n = 6$) | 7.4 \pm 12.3 ($n = 11$) | 68.6 \pm 0.3 ($n = 11$) |
| EC_{50} nicotine (μM \pm S.E.) | | | | |
| Control | 3.3 \pm 1.4* | 2.6 \pm 1.3 | 1.7 \pm 1.2* | |
| 1 μM nicotine incubation | 13.3 \pm 1.1* ($n = 6$) | 5.6 \pm 1.5 ($n = 7$) | 9.0 \pm 1.3* ($n = 5$) | |
| Hill slope ACh | | | | |
| Control | 1.1 \pm 0.1 | 1.0 \pm 0.3 | 0.5 \pm 2.0 | 1.8 \pm 3.0 |
| 1 μM nicotine incubation | 0.6 \pm 0.2 ($n = 8$) | 0.9 \pm 0.2 ($n = 6$) | 0.7 \pm 3.3 ($n = 11$) | 1.3 \pm 2.1 ($n = 11$) |
| Hill slope nicotine | | | | |
| Control | 1.6 \pm 0.7 | 1.5 \pm 0.7* | 1.6 \pm 0.4 | |
| 1 μM nicotine incubation | 1.4 \pm 0.2 ($n = 6$) | 1.1 \pm 0.4* ($n = 7$) | 1.3 \pm 0.4 ($n = 5$) | |

traces). After chronic nicotine treatment all three subunit ratios exhibited a reduced state of activation as evidenced by a significant reduction in their respective peak currents (Table I). Furthermore, after chronic nicotine exposure the 2 $\alpha 4$:3 $\beta 2$ subunit ratio displayed a significant increase in the EC_{50} value for ACh, whereas 1 $\alpha 4$:4 $\beta 2$ and 4 $\alpha 4$:1 $\beta 2$ subunit ratios showed a significant increase in the nicotine EC_{50} values (Fig. 4 and Table I). The 2 $\alpha 4$:3 $\beta 2$ subunit ratio was the only one that displayed a statistically significant reduction in the Hill coefficient after chronic exposure to nicotine.

$\alpha 4\beta 2$ Up-regulation and Subunit Ratio—Whole-mount immunofluorescence assays for the detection of surface $\alpha 4$ subunit and confocal imaging were performed to determine the effect of chronic nicotine exposure on the up-regulation of oocytes injected with different $\alpha 4$: $\beta 2$ subunit mRNA ratios. Oocytes were paired according to their similar current profile (*i.e.* no more than a 400-nA difference); oocytes incubated for 24 h with 1.0 μM nicotine were compared with oocytes without nicotine exposure. Fig. 5 illustrates representative confocal sections of immunolabeled $\alpha 4$ subunit on the surface membranes

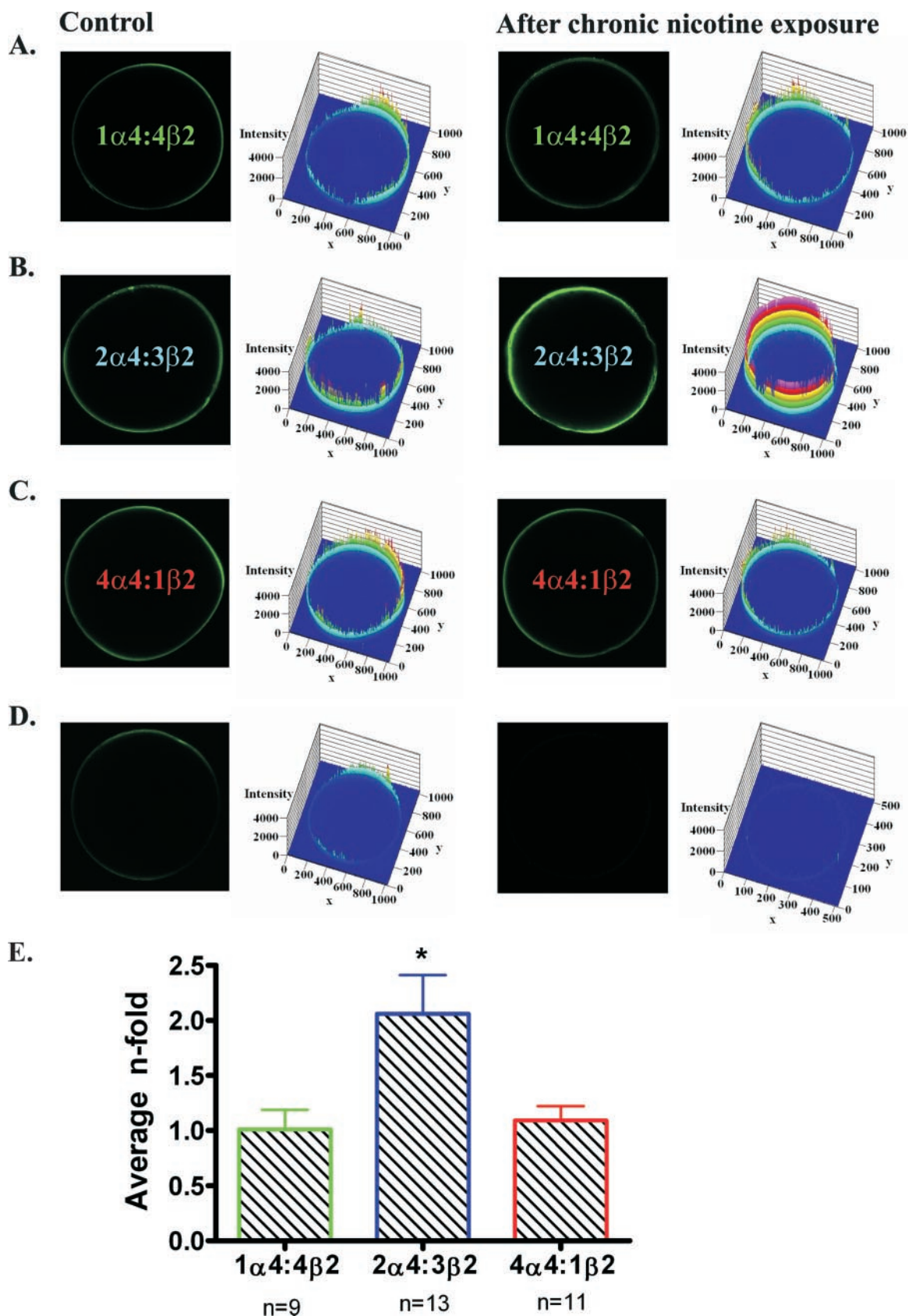


FIG. 5. Confocal images of the immunofluorescence surface detection of the $\alpha 4$ subunit after chronic nicotine exposure. *A*, fluorescence intensity of oocytes injected with $1\alpha 4:4\beta 2$ subunit ratio (Gain 840). The initial responses at $300 \mu\text{M}$ ACh for the incubated and non-incubated oocytes were 228 nA and 190 nA, respectively. *B*, fluorescence intensity of oocytes injected with $2\alpha 4:3\beta 2$ ratio (Gain 840). The initial response at $300 \mu\text{M}$ ACh for the incubated oocyte was 3333 nA and 2834 nA for the non-incubated oocyte. *C*, fluorescence intensity of oocytes injected with $4\alpha 4:1\beta 2$ ratio (Gain 840). The initial responses at $300 \mu\text{M}$ ACh for the incubated and non-incubated oocytes were 2240 nA and 3027 nA, respectively. *D*, fluorescence intensity of oocyte not injected with any $\alpha 4/\beta 2$ subunit ratio but treated with primary and secondary antibodies (*left*). Oocyte injected with $1\alpha 4:4\beta 2$ (160 nA) but not treated with primary antibody (*right*). *E*, the average *n*-fold changes are presented as bar graphs for each $\alpha 4/\beta 2$ subunit ratio ($1\alpha 4:4\beta 2$ in green, $2\alpha 4:3\beta 2$ in blue, and $4\alpha 4:1\beta 2$ in red). *, $p < 0.05$.

TABLE II

Effect of chronic nicotine exposure on membrane nAChR expression in oocytes injected with different $\alpha 4\beta 2$ subunit ratios

We used the threshold function to eliminate all the pixels contributing to background noise. The Total intensity value reported corresponds to the summation of all fluorescence intensity values in *X* and *Y* coordinates for each optical slice. *n*-fold is the intensity ratio of post nicotine incubation to pre-nicotine incubation.

| Oocyte | Total intensity | | <i>n</i> -fold |
|---|-----------------|-------------------|----------------|
| | Control | Nicotine exposure | |
| 1$\alpha 4$:4$\beta 2$ Subunit ratio | | | |
| A | 32,653,452 | 18,977,688 | 0.6 |
| B | 25,713,198 | 34,708,271 | 1.3 |
| C | 37,475,517 | 65,919,632 | 1.8 |
| D | 71,718,876 | 22,260,347 | 0.3 |
| E | 70,138,747 | 34,817,910 | 0.5 |
| F | 39,093,480 | 59,029,584 | 1.5 |
| G | 54,066,932 | 29,547,749 | 0.5 |
| H | 12,780,008 | 16,890,072 | 1.3 |
| I | 12,762,198 | 17,020,889 | 1.3 |
| 2$\alpha 4$:3$\beta 2$ Subunit ratio | | | |
| A | 37,409,955 | 89,524,470 | 2.4 |
| B | 20,140,013 | 35,433,111 | 1.8 |
| C | 26,675,278 | 18,403,306 | 0.7 |
| D | 16,751,488 | 23,428,986 | 1.4 |
| E | 11,254,099 | 24,304,366 | 2.2 |
| F | 7,161,556 | 10,972,231 | 1.5 |
| G | 12,288,492 | 62,266,016 | 5.1 |
| H | 12,521,833 | 50,045,824 | 4.0 |
| I | 21,012,553 | 54,983,787 | 2.6 |
| J | 15,213,627 | 28,738,285 | 1.9 |
| K | 32,013,197 | 29,251,917 | 0.9 |
| L | 29,680,699 | 33,778,561 | 1.1 |
| M | 23,657,396 | 28,404,875 | 1.2 |
| 4$\alpha 4$:1$\beta 2$ Subunit ratio | | | |
| A | 51,979,117 | 34,598,248 | 0.7 |
| B | 36,506,476 | 46,222,295 | 1.3 |
| C | 27,975,433 | 56,847,910 | 2.0 |
| D | 53,919,907 | 41,525,166 | 0.8 |
| E | 29,298,139 | 24,899,972 | 0.8 |
| F | 22,038,054 | 19,785,492 | 0.9 |
| G | 32,201,442 | 26,111,141 | 0.8 |
| H | 13,628,157 | 14,255,826 | 1.0 |
| I | 15,243,628 | 15,707,613 | 1.0 |
| J | 9,991,802 | 18,202,873 | 1.8 |
| K | 14,558,918 | 12,398,914 | 0.9 |

and their corresponding fluorescence intensity profiles for each of the three subunit ratios studied. The total fluorescence intensity for each condition was calculated as explained under "Experimental Procedures." Table II shows the $\alpha 4$ fluorescence intensity originating from the plasma membrane of oocytes before and after chronic nicotine exposure for the three subunit ratios. The *n*-fold values presented in Table II correspond to the intensity after chronic nicotine exposure divided by the intensity before chronic nicotine exposure. *n*-fold values did not reveal a consistent increase or decrease for the 1 $\alpha 4$:4 $\beta 2$ and 4 $\alpha 4$:1 $\beta 2$ subunit ratios, thus indicating that there was no obvious change in the fluorescence intensity of the $\alpha 4$ subunit before and after chronic nicotine exposure (Fig. 5, A and C, respectively). A plot of the average *n*-fold values for the three subunit ratios studied is shown in Fig. 5E. The average *n*-fold values were 1.0 ± 0.2 and 1.1 ± 0.1 for the 1 $\alpha 4$:4 $\beta 2$ and 4 $\alpha 4$:1 $\beta 2$ subunit ratios, respectively. In contrast, the average *n*-fold value for the 2 $\alpha 4$:3 $\beta 2$ subunit ratio of 2.1 ± 0.4 was significantly different from the other two subunit ratios ($p = 0.0119$). This significant increase in the average *n*-fold was consistent with the robust increment in the fluorescence intensity observed for the $\alpha 4$ subunit (Fig. 5B, right). These results indicate that 2 $\alpha 4$:3 $\beta 2$ was the only subunit ratio that clearly up-regulated after chronic nicotine exposure and suggest that the subunit ratio of the $\alpha 4\beta 2$ nAChR is critical for the nicotine-induced up-regulation.

DISCUSSION

The results presented here demonstrate that the functional state of the $\alpha 4\beta 2$ nAChR in the surface membrane of *Xenopus* oocytes can be manipulated by injecting different subunit ratios of mRNAs encoding for these two nAChR subunits. Our data are consistent with previous studies (29–31) and clearly demonstrate that the functional properties of the $\alpha 4\beta 2$ neuronal nAChR depend on the heteropentamer subunit ratio.

Functional and Structural Implications of Subunit Ratios—The optical density data presented in Fig. 1 indicate that the proportion of α subunit in the oocyte membrane increases as the ratio of α/β injected increases. In addition, the electrophysiological data shown establish a marked difference in function for each of the subunit ratios studied. It is thus reasonable to hypothesize that functional heteropentamers of different stoichiometries, 4 $\alpha 4$:1 $\beta 2$, 3 $\alpha 4$:2 $\beta 2$, 2 $\alpha 4$:3 $\beta 2$, and 1 $\alpha 4$:4 $\beta 2$, were assembled in the plasma membrane of oocytes injected with different $\alpha:\beta$ subunit ratios. Moreover, it is possible that a heterogeneous population of the previously mentioned stoichiometries is present on any given oocyte injected with either of the subunit ratios. Although we recognize that as a plausible scenario based on the increase in $\alpha 4$ subunit on the oocyte plasma membrane as a function of $\alpha 4$ subunit injected and the distinct electrophysiological data for each subunit ratio injected, we hypothesize that at least one $\alpha 4\beta 2$ stoichiometry is favored for each of the subunit ratios injected.

It has been proposed that ($\alpha 4$)₂($\beta 2$)₃ is the predominant stoichiometry in the central nervous system (27, 28). Previous studies have shown that $\alpha 4$ expressed alone does not form active nAChR channels (30); therefore, functional heteropentameric $\alpha 4\beta 2$ nAChRs presumably contain at least two agonist binding sites and are likely to be located at the $\alpha 4$ - $\beta 2$ subunit interface. For these putative heteropentamers, the number of agonist binding sites (*i.e.* $\alpha 4$ - $\beta 2$ subunit interfaces) may control the degree of ion channel activation. We found that the amount of ACh-induced macroscopic current increased proportional to the amount of $\alpha 4$ subunit detected in the plasma membrane of the oocyte. This result was consistent for the 1 $\alpha 4$:4 $\beta 2$ and 2 $\alpha 4$:3 $\beta 2$ subunit ratios given that the corresponding hypothetical numbers of symmetric agonist binding sites ($\alpha 4$ - $\beta 2$ sites) are 1 and 2, respectively, and their corresponding peak currents are 211 ± 28 nA and 522 ± 99 nA. It is noteworthy that the 4 $\alpha 4$:1 $\beta 2$ subunit ratio displayed the largest macroscopic current and is the only subunit ratio displaying two EC₅₀ values for ACh (4.0 and 52.2 μ M). These results lead to the hypothesis that the large currents observed for 4 $\alpha 4$:1 $\beta 2$ could be caused by an increase in the fraction of functional receptors or a larger unitary conductance when compared with the other subunit ratios. Interestingly, the EC₅₀ value for nicotine activation was not significantly affected as the amount of $\alpha 4$ subunit was increased, yet there was a significant increase in the peak currents as a function of $\alpha 4$ subunit. These results suggest that the properties of agonist binding for $\alpha 4\beta 2$ channel activation might have distinct dynamics or perhaps structural requirements for ACh and nicotine. In contrast to the nicotine-induced activation of the $\alpha 4\beta 2$ nAChR, which appears to be independent of the subunit ratio expressed on the oocyte surface, desensitization was remarkably affected by acute nicotine exposure. The aforementioned results suggest that activation and desensitization of the $\alpha 4\beta 2$ nAChR by nicotine could be triggered by two independent mechanisms, which in turn suggest the possibility of at least two distinct binding sites for nicotine.

ACh produced a small activation of 1 $\alpha 4$:4 $\beta 2$ subunit ratio; this is consistent with the presence of a predominant stoichiometry ($\alpha 4$)₁($\beta 2$)₄ or a problem of receptor assembly. It is note-

worthy that the dose-response curve for nicotine shows a biphasic profile for the $1\alpha 4:4\beta 2$ and $2\alpha 4:3\beta 2$ subunit ratios at 0.1, 1, 3, 10, 30, 100, and 300 μM (Fig. 4, lower panel in blue), consistent with a previous study (14). This previous study proposed that desensitization was responsible for the biphasic shape of the dose-response curve. In contrast, we found that the $4\alpha 4:1\beta 2$ subunit ratio only displays this biphasic behavior with nicotine concentrations higher than 300 μM .

Subunit Ratio Versus Desensitization and Chronic Up-regulation—Desensitization of the $\alpha 4\beta 2$ nAChR induced by acute exposure to nicotine (0.3, 1.0, or 10 μM ; see Fig. 2, A–F) increased as the ratio of the $\beta 2/\alpha 4$ subunit increased in the oocyte surface membrane. These results are consistent with previous work suggesting that the $\beta 2$ subunit controls the desensitization of the $\alpha 4\beta 2$ nAChR (34). In theory, if the proportion of subunits expressed in the surface membrane is linearly proportional to the most abundant stoichiometry, only the $1\alpha 4:4\beta 2$ and $2\alpha 4:3\beta 2$ subunit ratios will contain both $\alpha 4$ - $\beta 2$ and $\beta 2$ - $\beta 2$ subunit contacts. Along the same hypothetical assumption, the $4\alpha 4:1\beta 2$ subunit ratio, which produced the largest macroscopic currents, would not contain $\beta 2$ - $\beta 2$ contacts but only one $\alpha 4$ - $\beta 2$ contact. The present data are consistent with these hypothetical assumptions given that the $1\alpha 4:4\beta 2$ and $2\alpha 4:3\beta 2$ subunit ratios, which have $\beta 2$ - $\beta 2$ contacts, displayed a remarkable nicotine-induced desensitization (Fig. 2E) and a distinct biphasic dose-response curve for nicotine. In contrast, the $4\alpha 4:1\beta 2$ subunit ratio shows a biphasic dose-response curve for nicotine at higher nicotine concentrations and displays a remarkable resistance to desensitization. Based on these results we hypothesize that intersubunit contacts involving $\beta 2$ subunits control the allosteric interactions, which govern the conformational transition to the desensitized state. In theory, this biphasic profile could be consistent with the presence of two different binding sites for nicotine: one activation site and a second binding site promoting receptor desensitization. In this hypothetical model, the site responsible for nicotine-induced activation of the $\alpha 4\beta 2$ nAChR has different dynamics and/or structural requirements from the site that promotes receptor desensitization. Nevertheless, more experimental data are needed to further test this hypothetical model.

After chronic nicotine exposure there was a loss in function in all three subunit ratios, shown by the decrease in peak current and the shift of EC_{50} values toward higher agonist concentrations. The most significant increase in EC_{50} for ACh was observed in oocytes expressing $2\alpha 4:3\beta 2$ subunit ratio, whereas the $1\alpha 4:4\beta 2$ and $4\alpha 4:1\beta 2$ subunit ratios displayed a significant increase in their nicotine EC_{50} values (Table I). Remarkably, only oocytes expressing the $2\alpha 4:3\beta 2$ subunit ratio clearly up-regulated after chronic nicotine exposure (Fig. 5), suggesting that the subunit ratio is critical for the nicotine-induced up-regulation of this neuronal nAChR.

The results presented here clearly indicate that the functional state of the $\alpha 4\beta 2$ nAChR is regulated by subunit ratio. Previous studies addressing $\alpha 4\beta 2$ up-regulation did not consider the importance of subunit stoichiometry (10, 13, 16, 22,

26, 35–37). Our results also suggest that nicotine-induced desensitization and up-regulation of this neuronal nicotinic receptor appears to be remarkably defined by very specific interactions between the neuronal nicotinic subunits. Given that the $\alpha 4\beta 2$ nAChR is wide spread in brain presynaptic terminals, it is reasonable to consider that control of the subunit ratios of these heteropentamer receptors could regulate neurotransmitter release in the central nervous system and nicotine sensitivity in humans.

Acknowledgments—We thank Drs. Carlos González, Amelia Rivera, and Eduardo Rosa-Molinari for valuable technical assistance. In addition, we thank Dr. Enrique Ochoa for kind input on the manuscript.

REFERENCES

1. Role, L. W. (1992) *Curr. Opin. Neurobiol.* **2**, 254–262
2. Sargent, P. B. (1993) *Annu. Rev. Neurosci.* **16**, 403–443
3. Dani, J. A., and Heinemann, S. (1996) *Neuron* **16**, 905–908
4. Lindstrom, J. (1997) *Mol. Neurobiol.* **15**, 193–222
5. Changeux, J. P., and Edelman, S. J. (1998) *Neuron* **21**, 959–980
6. Marks, M. J., Burch, J. B., and Collins, A. C. (1983) *J. Pharmacol. Exp. Ther.* **226**, 817–825
7. Benwell, M. E., Balfour, D. J., and Anderson, J. M. (1988) *J. Neurochem.* **50**, 1243–1247
8. Flores, C. M., Rogers, S. W., Pabreza, L. A., Wolfe, B. B., and Kellar, K. J. (1992) *Mol. Pharmacol.* **41**, 31–37
9. Breese, C. R., Marks, M. J., Logel, J., Adams, C. E., Sullivan, B., Collins, A. C., and Leonard, S. (1997) *J. Pharmacol. Exp. Ther.* **282**, 7–13
10. Whiteaker, P., Sharples, C. G., and Wonnacott, S. (1998) *Mol. Pharmacol.* **53**, 950–962
11. Lukas, R. J. (1991) *J. Neurochem.* **56**, 1134–1145
12. Marks, M. J., Grady, S. R., and Collins, A. C. (1993) *J. Pharmacol. Exp. Ther.* **266**, 1268–1276
13. Peng, X., Gerzanich, V., Anand, R., Whiting, P. J., and Lindstrom, J. (1994) *Mol. Pharmacol.* **46**, 523–530
14. Vibat, C. R., Lasalde, J. A., McNamee, M. G., and Ochoa, E. L. (1995) *Cell. Mol. Neurobiol.* **15**, 411–425
15. Hsu, Y. N., Amin, J., Weiss, D. S., and Wecker, L. (1996) *J. Neurochem.* **66**, 667–675
16. Eilers, H., Schaeffer, E., Bickler, P. E., and Forsayeth, J. R. (1997) *Mol. Pharmacol.* **52**, 1105–1112
17. Fenster, C. P., Rains, M. F., Noerager, B., Quick, M. W., and Lester, R. A. (1997) *J. Neurosci.* **17**, 5747–5759
18. Sharp, B. M., and Beyer, H. S. (1986) *J. Pharmacol. Exp. Ther.* **238**, 486–491
19. Lapchack, P. A., Araujo, D. M., Quirion, R., and Collier, B. (1989) *J. Neurochem.* **52**, 483–491
20. Ke, L., Eisenhour, C. M., Bencherif, M., and Lukas, R. J. (1998) *J. Pharmacol. Exp. Ther.* **286**, 825–840
21. Schwartz, R. D., and Kellar, K. J. (1985) *J. Neurochem.* **45**, 427–433
22. Fenster, C. P., Whitworth, T. L., Sheffield, E. B., Quick, M. W., and Lester, R. A. (1999) *J. Neurosci.* **19**, 4804–4814
23. Quick, M. W., and Lester, R. A. (2002) *J. Neurobiol.* **53**, 457–478
24. Wonnacott, S. (1990) *Trends Pharmacol. Sci.* **11**, 216–219
25. Balfour, D. J. (1994) *Addiction* **89**, 1419–1423
26. Buisson, B., and Bertrand, D. (2001) *J. Neurosci.* **21**, 1819–1829
27. Anand, R., Conroy, W. G., Schoepfer, R., Whiting, P., and Lindstrom, J. (1991) *J. Biol. Chem.* **266**, 11192–11198
28. Cooper, E., Couturier, S., and Ballivet, M. (1991) *Nature* **350**, 235–238
29. Papke, R. L., Boulter, J., Patrick, J., and Heinemann, S. (1989) *Neuron* **3**, 589–596
30. Zwart, R., and Vijverberg, H. P. (1998) *Mol. Pharmacol.* **54**, 1124–1131
31. Nelson, M. E., Kuryatov, A., Choi, C. H., Zhou, Y., and Lindstrom, J. (2003) *Mol. Pharmacol.* **63**, 332–341
32. Ohlsson, R. I., Lane, C. D., and Guengerich, F. P. (1981) *Eur. J. Biochem.* **115**, 367–373
33. Sharples, C. G., and Wonnacott, S. (2001) *Toxic Reviews* **19**, 1–12
34. Bohler, S., Gay, S., Bertrand, S., Corring, P. J., Edelman, S. J., Changeux, J. P., and Bertrand, D. (2001) *Biochemistry* **40**, 2066–2074
35. Bencherif, M., Fowler, K., Lukas, R. J., and Lippello, P. M. (1995) *J. Pharmacol. Exp. Ther.* **275**, 987–994
36. Gopalakrishnan, M., Molinari, E. J., and Sullivan, J. P. (1997) *Mol. Pharmacol.* **52**, 524–534
37. Harkness, P. C., and Millar, N. S. (2002) *J. Neurosci.* **22**, 10172–10181